

Visible Light Promoted Hydrochlorination of Olefin Over Pt, Au and Pd Supported on Zirconia

Xuzhuang Yang · Huaiyong Zhu · Guanjin Gao ·
Chenhui Han · Jie Wang · Jie Liu ·
Huailiang Lu · Min Tong · Xiaoyuan Liang

Received: 13 October 2013 / Accepted: 23 October 2013 / Published online: 5 November 2013
© Springer Science+Business Media New York 2013

Abstract The Pt, Au and Pd catalysts supported on zirconia were prepared by the colloid deposition method. The catalytic activities of the catalysts for the hydrochlorination of 4-phenyl-1-butene were investigated under the irradiation of visible light, taking hydrochloric acid as the sources of chloride and hydrogen. The catalysts exhibited superior activities under the irradiation, giving rise to 4-phenylbutyl chloride and 4-phenyl-2-butenol, but they were almost inactive without the irradiation. Ethanol was unfavorable to the reaction. In addition to 4-phenylbutyl chloride, 2,3-dimethylstyrene was the by-product on the Pt and Au catalysts, and the isomerization from 4-phenyl-1-butene to benzene-1-butenyl occurred on the Pd/ZrO₂ catalyst in ethanol solution.

Keywords Alkenes · Photocatalysis · Hydrochlorination · Noble metal

1 Introduction

The addition of hydrogen halide to olefins is one of the fundamental reactions in organic chemistry [1, 2]. But the hydrochlorination of olefins, especially the addition of HCl

to olefins, only occurs at a useful rate to strained, highly substituted or part of a styryl system [2–4]. Gaspar and Carreira [1] have studied a series of hydrochlorination reactions using the Co catalyst at the room temperature in the ethanol solution. The sources of hydrogen and chloride are from PhSiH₃ and *para*-toluenesulfonyl chloride (TsCl), respectively. Taking hydrochloric acid as the sources of hydrogen and chloride and promoting the hydrochlorination process by visible light on supported noble metal catalysts has seldom been studied.

Zirconia is a semiconductor, and the energy of its band gap is about 5.0 eV [5], much larger than the energies of the photons of visible light. Zirconia is widely used as a photocatalyst in the production of hydrogen from water [6], the oxidation of 2-propanol to acetone [7], the oxidation of propene [8], oxidations of methanol and hexane [9] etc. Supported Pt, Au and Pd nanoparticles have usually been used in the photocatalytic processes such as the degradation of pollutants [10, 11], the hydrogen production from water or methanol [12–15], and the selective oxidations [16, 17] in recent years due to their good photocatalytic performance and chemical inertness towards the photo oxidation [18]. Noble metal nanoparticles supported on a semiconductor do not form a part of the framework of the support, but are in a separate phase in the interfacial contact with the support. The electron transfer occurs between the noble metal nanoparticles and the semiconductor under irradiation [17, 18], which enhances the redox capabilities of the active sites on the semiconductor or on the noble metal nanoparticles and thus improves the photocatalytic performance. Electrons are supposed to transfer from noble metal to the conduction band of the semiconductor under the irradiation of visible light, by which oxidative sites form on the noble metal nanoparticles and reductive sites form on the surface of the semiconductor [17, 18]. But they

X. Yang (✉) · G. Gao · C. Han · J. Wang · J. Liu · H. Lu ·
M. Tong · X. Liang
School of Chemistry and Chemical Engineering, Inner Mongolia
University, Hohhot, Inner Mongolia 010021, People's Republic
of China
e-mail: xzyang2007@yahoo.com

H. Zhu
School of Physical and Chemical Sciences, Queensland
University of Technology, Brisbane, QLD 4001, Australia
e-mail: hy.zhu@qut.edu.au

transfer reversely under the irradiation of UV light, reducing the recombination of the photoexcited electrons and holes on the surface of the semiconductor [10, 12, 14, 19]. The surface plasmon resonance (SPR) often occurs on supported noble metal nanoparticles under the irradiation of light, which is believed to be capable of inducing or promoting some reactions [16, 18, 20].

In this study, the catalysts of gold, platinum and palladium nanoparticles supported on zirconia were prepared by the metal colloid deposition method. The photocatalytic activities of the catalysts for the hydrochlorination of 4-phenyl-1-butene were investigated under the irradiation of visible light. The aims are to study the influence of visible light on the activities of the catalysts and the product distribution of the reaction.

2 Experimental

In a general procedure, 2.5 g of zirconia powder was dispersed in 100 ml of the $\text{HAuCl}_4 \cdot 3\text{H}_2\text{O}$, $\text{H}_2\text{PtCl}_6 \cdot x\text{H}_2\text{O}$ or PdCl_2 solution with a specific concentration, followed by adding 20 ml of the 0.53 M lysine solution in the suspension with vigorous stirring for 30 min. Then, 10 ml of the 0.35 M sodium borohydride solution was added portion-wise followed by adding 10 ml of the 0.3 M hydrochloric acid solution, and continuously stirring for 24 h. The catalysts of noble metals supported on zirconia were then obtained by filtration, washing with deionized water and ethanol, and finally drying at 60 °C, labeled as Pt/ZrO_2 , Au/ZrO_2 and Pd/ZrO_2 . The nominal metal content in each catalyst was 1.5 wt%.

X-ray diffraction (XRD) measurements were performed using a Philips PANalytical X'Pert PRO diffractometer operating at 40 kV and 40 mA. The morphology of the catalyst was investigated by a Philips CM200 transmission electron microscope (TEM) employing an accelerating voltage of 200 kV. X-ray photoelectron spectroscopy (XPS) analysis was performed on a Kratos Analytical Axis Ultra X-ray photoelectron spectrometer. The diffuse reflectance UV–visible spectra (UV–Vis) of the samples were recorded on a Cary 5000 spectrometer.

The hydrochlorination reaction was conducted in a 50 ml round bottom flask connected with a reflux condenser at the atmospheric pressure at 60 °C. The outlet of the condenser was connected with a pressure balancing bag. In a general procedure, 2.5 ml of the pure 4-phenyl-1-butene and 10 ml of the hydrochloric acid solution (36.5 wt%) together with 100 mg of the catalyst were added in the flask with stirring, irradiating by incandescence light during the reaction. The products were qualified by a GC–MS and quantified by a GC–FID.

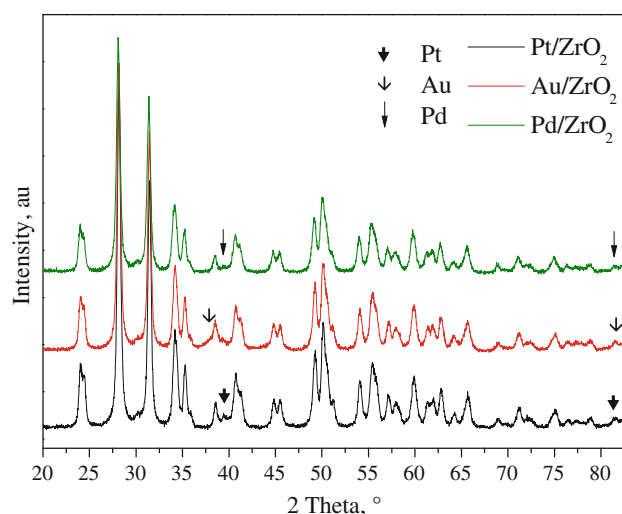


Fig. 1 XRD patterns of supported noble metal catalysts

3 Results

Figure 1 shows the XRD patterns of the catalysts. The diffraction intensity of the peaks from the noble metal in each sample is weak due to its high dispersion and low content (about 1.5 wt%). The weak diffraction peaks at $2\theta = 39.7^\circ$ and 81.2° in the pattern of the Pt/ZrO_2 catalyst are attributed to the diffractions of metallic Pt in the cubic phase. The shoulder at $2\theta = 38.1^\circ$ and the weak peak at $2\theta = 81.7^\circ$ in the pattern of the Au/ZrO_2 catalyst are attributed to gold in the cubic phase, and the weak peaks at $2\theta = 39.9^\circ$ and 81.6° in the pattern of the Pd/ZrO_2 catalyst are attributed to metallic Pd in the cubic phase. The diffractions from zirconia indicate that zirconia is in the monoclinic phase. The average crystal size of zirconia calculated by Scherrer's equation is about 20 nm, using the diffraction peak of the (-111) crystal faces of zirconia at $2\theta = 28.2^\circ$.

The TEM images of the catalysts are shown in Fig. 2. The sizes of the Pt, Au, and Pd nanoparticles on the surface of zirconia are almost similar and distribute in a very narrow range, with a diameter of about 5–6 nm. The TEM images of the three catalysts at a higher magnification indicate that no other noble metal species other than metallic nanoparticles in the three catalysts. The sizes of zirconia nanoparticles observed by TEM are about 20–30 nm, which is in consistent with the calculation from XRD.

The XPS results are shown in Fig. 3. The peaks of the binding energy at 83.9 and 87.7 eV in the pattern of Au are assigned to $\text{Au}4f_{7/2}$ and $\text{Au}4f_{5/2}$ of metallic gold, respectively; those at 71.2 and 74.4 eV in the pattern of Pt are assigned to $\text{Pt}4f_{7/2}$ and $\text{Pt}4f_{5/2}$ of metallic platinum, respectively; those at 335.5 and 341.0 eV in the pattern of Pd are assigned to $\text{Pd}3d_{5/2}$ and $\text{Pd}3d_{3/2}$ of metallic palladium, respectively. The peak at 332.5 eV in the pattern of

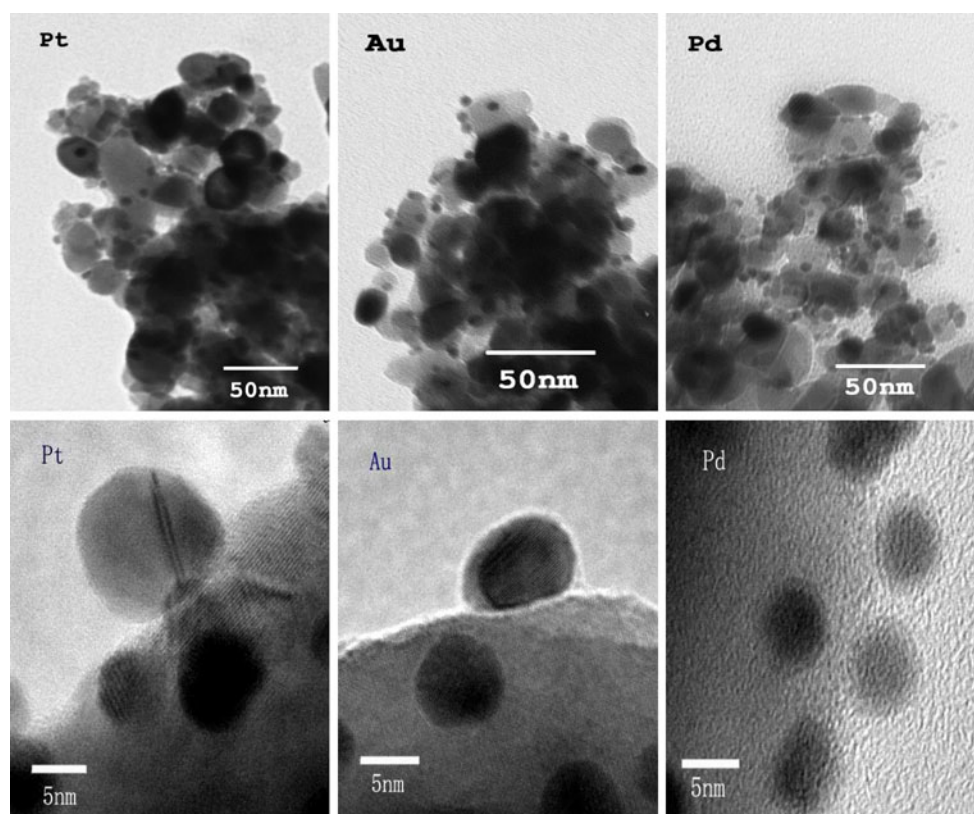


Fig. 2 TEM images of supported noble metal catalysts

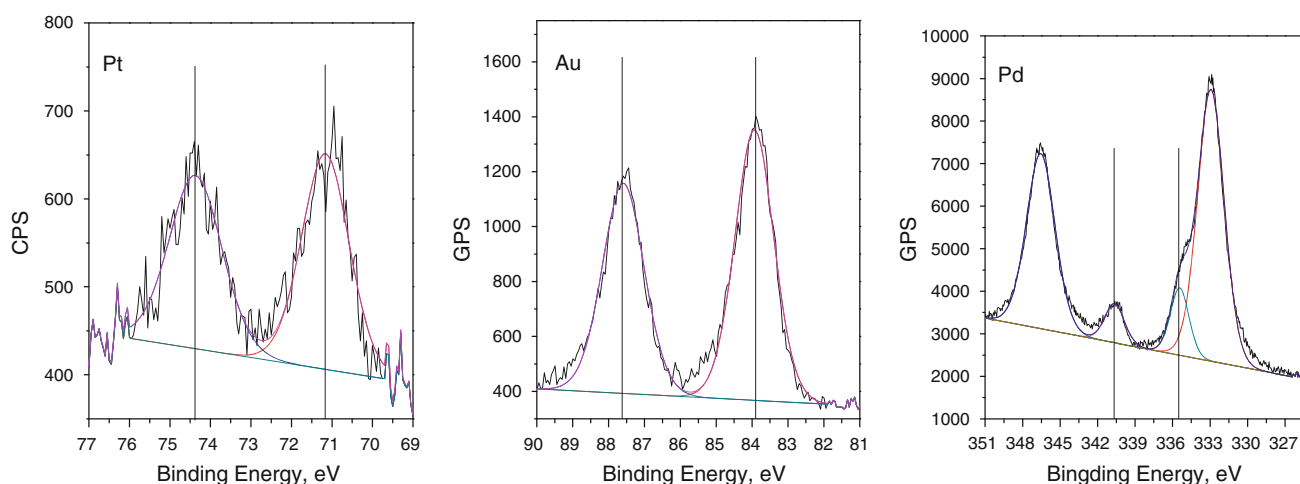


Fig. 3 XPS spectra of supported noble metal catalysts

Pd is attributed to $Zr3p_{3/2}$ of zirconia, which is overlapping with that of $Pd3d_{5/2}$ of metallic palladium. The XPS results indicate that noble metal species on zirconia are in metallic phases.

Figure 4 shows the UV–Vis spectra of the catalysts. Zirconia exhibits a weak absorption band from 400 to

250 nm, attributed to the electron transition from defect to conduction band, and a strong absorption band from 250 to 190 nm, corresponding to the transition of electrons from valance band to conduction band. Thus the band gap of this zirconia is 4.96 eV. All the three catalysts exhibit strong absorption bands from visible to UV regions, which can be

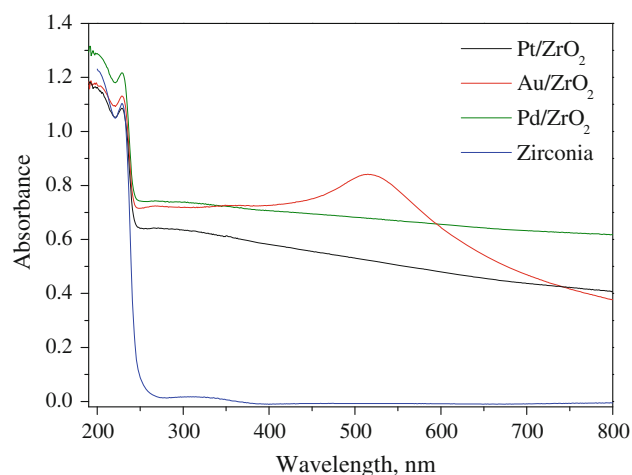


Fig. 4 UV-Vis spectra of supported noble metal catalysts

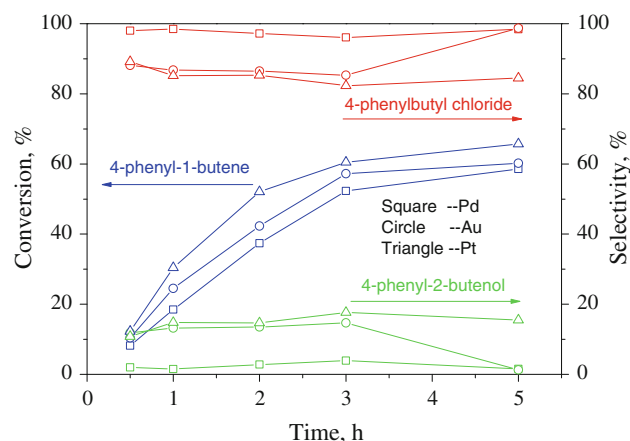


Fig. 5 Conversions and selectivities of Pt, Au and Pd catalysts

Table 1 Results of addition on noble metal supported catalysts (3 h, 60 °C, light strength, 1 w/cm²)

Catalyst	Irradiation			No irradiation			Irradiation in ethanol		
	Conversion (%)	Selectivity (%)		Conversion (%)	Selectivity (%)		Conversion (%)	Selectivity (%)	
		A	B		A	B		A	B
Blank	1.2	100	—	—	—	—	—	—	—
Zirconia	1.5	100	—	—	—	—	—	—	—
Pt/ZrO ₂	60.5	82.3	17.7	2.0	93.8	6.2	5.0	78.8	11.2 ^b
Au/ZrO ₂	57.2	85.3	14.7	4.5	92.6	7.4	1.2	55.0	45.0 ^b
Pd/ZrO ₂	52.3	96.1	3.9	3.1	93.7	6.3	15.8	100 ^a	0

A 4-phenylbutyl chloride, B 4-phenyl-2-butenol

^a Benzene, -1-butenyl

^b Benzene-4-ethenyl-1,2-dimethyl-

attributed to the interband and intraband transition of electrons in noble metal nanoparticles. The broad band peaking at 520 nm in the pattern of the Au/ZrO₂ catalyst is attributed to the SPR absorption of gold nanoparticles.

The addition results of 4-phenyl-1-butene in different conditions are listed in Table 1. The addition of 4-phenyl-1-butene occurred at a very slow rate, with a conversion of about 1.2 % in 3 h, only by irradiation at 60 °C (blank reaction). Zirconia was not active to this reaction under irradiation at 60 °C because the conversion on it was only 1.5 % which was comparative to that of the blank reaction. The product of the blank reaction and that on zirconia was solely 4-phenylbutyl chloride. The conversion on the noble metal supported catalysts increased slightly, from 2 to 4.5 % in 3 h, when the reaction was proceeded in dark at 60 °C, indicating these supported noble metal catalysts were not active in the thermal condition. The products in this condition were mainly 4-phenylbutyl chloride and a small amount of 4-phenyl-2-butenol. The conversion of 4-phenyl-1-butene in 3 h dramatically increased to 52.3–60.5 % for the three catalysts under the irradiation of

visible light. The selectivity of 4-phenylbutyl chloride decreased from about 93 to 82.3 % and 85.3 % for Pt/ZrO₂ and Au/ZrO₂, respectively, but increased from 93.7 to 96.1 % for Pd/ZrO₂, compared with the results of the thermal reaction.

The reaction was also investigated in an ethanol solution (Table 1). The reaction rates were dramatically retarded on all catalysts when ethanol was added in the reactor. The conversions of 4-phenyl-1-butene on Pt/ZrO₂, Au/ZrO₂ and Pd/ZrO₂ decreased to 5.0, 1.2 and 15.8 %, respectively. The main products are 4-phenylbutyl chloride and 2,3-dimethylstyrene (benzene, 4-ethenyl-1,2-dimethyl-) on Pt/ZrO₂ and Au/ZrO₂. However, the isomerization from 4-phenyl-1-butene to benzene, -1-butenyl- occurred on Pd/ZrO₂ in the ethanol solution, instead of the addition reaction. Benzene, -1-butenyl- was the only product of the isomerization reaction. The conversions of 4-phenyl-1-butene on the recovered catalysts decreased by about 20 %.

The results of time-on-stream of the three catalysts are shown in Fig. 5. The conversions of 4-phenyl-1-butene increased with time on the three catalysts. The Pt/ZrO₂

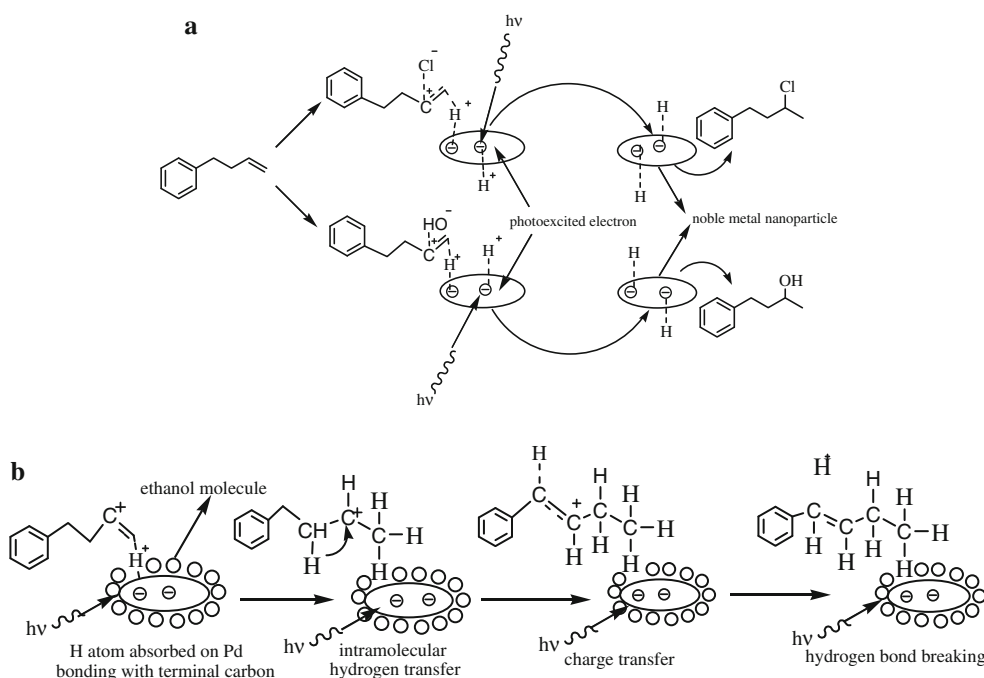


Fig. 6 Mechanisms of addition and isomerization on supported noble metal catalysts under irradiation of visible light

catalyst exhibited the best conversion but the poorest selectivity of 4-phenylbutyl chloride in 5 h. The Pd/ZrO₂ catalyst has the best selectivity of 4-phenylbutyl chloride during the reaction. The selectivity of 4-phenylbutyl chloride on the Au/ZrO₂ catalyst was lower than that on the Pd/ZrO₂ catalyst in 3 h but they are comparable in 5 h.

4 Discussion

The results above indicate that visible light promotes the addition reactions of an olefin on supported noble metal catalysts. The activities of the catalysts exhibit strong relations with the absorption of visible light by the noble metal nanoparticles on zirconia. The strong absorption bands from the visible region to the UV region by the Pt, Au and Pd nanoparticles indicate that electrons in the noble metal nanoparticles are excited by visible light and the interband and intraband transitions occur. The SPR can also occur on Au nanoparticles under irradiation in addition to the interband and intraband transitions. The electron transitions and the SPR result in active electrons on the surface of the noble metal nanoparticles. The active electrons on the surface of noble metals attract protons in the solution. The hydrogen atom absorbed on the surface of noble metal is readily to be added to the terminal carbon of the C=C group in the molecule of 4-phenyl-1-butene according to the Markovnikov rule [21]. A chloride anion or hydroxyl in the solution can be attracted by the

positively charged carbon to form the final products 4-phenylbutyl chloride or 4-phenyl-2-butenol. The addition mechanisms under irradiation of visible light on noble metal supported catalysts are shown in Fig. 6a.

Ethanol molecules surrounding the noble metal nanoparticles blocks most of the protons from reaching and being absorbed by the noble metal nanoparticles, making the reaction rate decrease dramatically. On the hand, some of the transition molecules containing positively charged carbon absorbed on noble metal nanoparticles cannot capture chloride ions or hydroxyls timely due to the blocking of ethanol molecules, as a result, they break into fragments under the attack of radicals in the solution or light. 2,3-dimethylstyrene is formed on Pt/ZrO₂ and Au/ZrO₂ in this condition. The photoexcited electrons on the surface of Pd nanoparticles might be less active than those on the surface of the Au or Pt nanoparticles, which cannot generate radicals to attack the transition molecules and thus the isomerization from 4-phenyl-1-butene to benzene, -1-butenyl- occurs due to the intramolecular hydrogen transfer [21]. The mechanism proposed is shown in Fig. 6b.

5 Conclusion

The catalysts of noble metal nanoparticles supported on zirconia exhibit superior activities for the hydrochlorination of 4-phenyl-1-butene using hydrochloric acid as the sources of chloride and hydrogen, which is regarded as a

reaction that is difficult to occur under usual thermal conditions, under the irradiation of visible light. The main products are 4-phenylbutyl chloride and 4-phenyl-2-butenol. The supported noble metal catalysts are almost inactive for the hydrochlorination reaction at 60 °C without irradiation. The activity of the catalyst is associated with the photoexcited electrons on the surfaces of the noble metal nanoparticles. Ethanol in the reaction system is unfavorable to the reaction because the ethanol molecules surrounding the noble metal nanoparticles block the hydrogen ions from reaching to their surfaces. In addition to 4-phenylbutyl chloride, another product is 2,3-dimethylstyrene on Pt/ZrO₂ and Au/ZrO₂, and the isomerization from 4-phenyl-1-butene to benzene, -1-butenyl occurred on Pd/ZrO₂ in ethanol solution.

Acknowledgments The work was financially supported by the key project of Inner Mongolia Education Department (NJZZ13002), the project of Grassland Talent of Inner Mongolia and the project of the western light from the ODPC of Inner Mongolia, and the Endeavour Australia Cheung Kong Research Fellowships.

References

1. Gaspar B, Carreira EM (2008) *Angew Chem Int Ed* 47:5758
2. Kropp PJ, Daus KA, Crawford SD, Tubergen MW (1990) *J Am Chem Soc* 112:7433
3. Bloch H, Pines H, Schmerling L (1946) *J Am Chem Soc* 68:153
4. Fahey RC, McPherson CA (1971) *J Am Chem Soc* 93:2445
5. Ganguly K, Sarkar S, Bhattacharyya S (1993) *J Chem Soc Chem Commun* 8:682
6. Sayama K, Arakawa H (1993) *J Phys Chem* 97:531
7. Navio J, Colón G (1994) *Stud Surf Sci Catal* 82:721
8. Pichat P, Herrmann JM, Disdier J, Mozzanega MN (1979) *J Phys Chem* 83:3122
9. Wu C, Zhao X, Ren Y, Yue Y, Hua W, Cao Y, Tang Y, Gao Z (2005) *J Mol Catal A* 229:233
10. Arabatzis I (2003) *J Catal* 220:127
11. Sakthivel S, Shankar M, Palanichamy M, Arabindoo B (2004) *Water Res* 38:3001
12. Bamwenda GR, Tsubota S, Nakamura T, Haruta M (1995) *J Photochem Photobiol A* 89:177
13. Gazsi A, Schubert G, Pusztai P, Solymosi F (2013) *Int J Hydrogen Energy* 38:7756
14. Rosseler O, Shankar MV, Du MK-L, Schmidlin L (2010) *J Catal* 269:179
15. Bowker M, James D, Stone P, Bennett R (2003) *J Catal* 217:427
16. Zhu H, Chen X, Zheng Z, Ke X (2009) *Chem Commun* 48:7524
17. Tanaka A, Hashimoto K, Kominami H (2011) *Chem Commun* 47:10446
18. Primo A, Corma A, Garcia H (2011) *Phys Chem Chem Phys* 13:886
19. Li X, Li F (2001) *Environ Sci Technol* 35:2381
20. Kowalska E, Mahaney OO, Abe R, Ohtani B (2010) *Phys Chem Chem Phys* 12:2344
21. Sergeev GB, Smirnov V, Rostovshchikova T (1983) *Russ Chem Rev* 52:259